High-field charge transport on the surface of Bi_2Se_3

M. Q. Weng* and M. W. Wu†

Hefei National Laboratory for Physical Sciences at Microscale and Department of Physics, University of Science and Technology of China, Hefei, Anhui 230026, China

(Received 30 June 2014; revised manuscript received 11 August 2014; published 10 September 2014)

We present a theoretical study on the high-field charge transport on the surface of Bi_2Se_3 and reproduce all the main features of the recent experimental results, i.e., the incomplete current saturation and the finite residual conductance in the high applied field regime [Costache *et al.*, Phys. Rev. Lett. **112**, 086601 (2014)]. Due to the hot-electron effect, the conductance decreases and the current shows a tendency of saturation with the increase of the applied electric field. Moreover, the electric field can excite carriers within the surface bands through interband precession and leads to a higher conductance. As a joint effect of the hot-electron transport and the carrier excitation, the conductance approaches a finite residual value in the high-field regime and the current saturation becomes incomplete. We thus demonstrate that, contrary to the conjecture in the literature, the observed transport phenomena can be understood qualitatively in the framework of surface transport alone. Furthermore, if a constant bulk conductance which is insensitive to the field is introduced, one can obtain a good quantitative agreement between the theoretical results and the experimental data.

DOI: 10.1103/PhysRevB.90.125306 PACS number(s): 73.50.Fq, 75.70.Tj, 72.25.Rb

I. INTRODUCTION

Three-dimensional topological insulators (TIs) have attracted much attention recently due to the intriguing fundamental physics as well as the possible application in TI devices [1–13]. A TI has a gapped insulating bulk but gapless conducting surface states, whose low energy ones can be described as massless Dirac fermions. The discovery of strong TI materials such as Bi_2Se_3, which has a bulk gap on the order of 300 meV, is of particular interest since it indicates the feasibility of room temperature devices. The surface states of strong TI materials near the Dirac points have been experimentally measured by spin-angle resolved photoemission spectroscopy [3,8]. However, the signature of the surface states has yet to be separated from the bulk ones in the transport experiments. Due to the relatively small gap, it is commonly believed that the bulk states have strong influence on the charge transport [7,14–22], even when the Fermi level resides inside the bulk gap [22–24]. However, without a clear understanding of surface transport, it is premature to distinguish the surface transport from the bulk one.

Recently, Costache *et al.* reported the experimental investigation of charge transport on the surface of Bi_2Se_3 under high electric fields [24]. In the experiment, it is observed that the current increases with the applied voltage in the low voltage regime, then shows a tendency of saturation in the intermediate regime. However, the current saturation is not complete. When the voltage further increases to about 50 mV, the current rises again. For conductance, it undergoes a slight change in the small voltage regime, then a quick reduction in the intermediate one, and finally saturates in the high applied voltage regime (larger than 50 mV). The current saturation or the conductance reduction is attributed to the inelastic electron–optical-phonon scattering in the surface states. The finite saturated conductance in the high voltage regime, however, is speculated to be the contribution from the bulk ones. It is argued that due to band bending, the energy gap of Bi_2Se_3 is reduced to 50 meV from the original 300 meV. Therefore, when the applied voltage is higher than 50 mV, the carriers are excited from surface bands to the bulk band which has finite conductance [24]. This argument is valid only when the transport is nearly ballistic so that the carriers in the surface bands can have enough energy gain to be excited to the bulk bands. However, for the diffusive transport in the experimental setup, the average energy gain is estimated to be less than 4 meV when the applied voltage is 50 mV. This indicates that the excitation of carriers from the surface bands to the bulk one is very unlikely to have significant effect on the transport even if the energy gap is indeed reduced to 50 meV. Therefore, the incomplete saturation and the finite residual conductance are unlikely to be from the bulk contribution.

Theoretically, the charge and spin transports of the surface state in Bi_2Se_3 have been investigated [14–17] with most of the studies focusing on the linear transport regime. Zhang and Wu have carried out a study on hot-electron transport under strong electric field of the surface states in Bi_2Se_3 by solving the kinetic spin Bloch equations (KSBEs) [25]. It is shown that the mobility, and hence the conductance, decreases with increasing applied electric field due to the hot-electron effect. Moreover, it is further shown that the electric field can excite carriers on the surface from the valance band to the conduction band through the interband precession. The excited carriers also contribute to the charge transport, thus leading to an enhanced conductance. Combining these two results, it is possible to understand the qualitative dependence of the current and the conductance on the applied voltage within the framework of the surface transport *alone*. In this paper, we show that the main features of the experimental results, i.e., the incomplete current saturation and the finite residual conductance, can indeed be captured by the surface transport *alone*, even though the bulk does have some non-negligible contribution to the total conductance.

This paper is organized as follows: In Sec. II, we set up the model and present the KSBEs. In Sec. III, we show

*weng@ustc.edu.cn
†mwwu@ustc.edu.cn

that the main features of the experimental results, such as the incomplete saturation of current and the finite residual conductance under high applied field, can be captured by the surface transport alone. Moreover, we show that one can obtain a good agreement between the experimental results and theoretical calculation by introducing a constant bulk conductance that does not change with the applied voltage. We summarize in Sec. IV

II. MODEL AND KSBEs

The Hamiltonian for the electrons on the (001) Bi_2Se_3 surface grown along the z direction is composed of the free part H_0 and the interacting part H_I. The free part describes the low energy surface states around the Γ point and can be written in form of the Rashba [26] spin-orbit coupling [2,27,28],

$$H_0 = \sum_k v_F(\mathbf{k}\times\hat{\mathbf{z}})\cdot\boldsymbol{\sigma}c^\dagger_{\mathbf{k}\sigma}c_{\mathbf{k}\sigma}, \tag{1}$$

in which $\hbar$ is set to 1, v_F is the Fermi velocity which is chosen to be 2×10^5 m/s [15], $c_{\mathbf{k}\sigma}$ ($c^\dagger_{\mathbf{k}\sigma}$) is the annihilation (creation) operator of the electron with in-plane momentum $\mathbf{k}=(k_x,k_y)$ and spin $\sigma=(\uparrow,\downarrow)$, and $\boldsymbol{\sigma}=(\sigma_x,\sigma_y,\sigma_z)$ are the Pauli matrices for spin. In the collinear spin space spanned by the eigenstates of σ_z ($|\uparrow\rangle$ and $|\downarrow\rangle$), the surface states can be expressed by the two helix spin states,

$$|\mathbf{k}\lambda\rangle = \sum_\sigma U_{\sigma\lambda}(\mathbf{k})|\mathbf{k}\sigma\rangle. \tag{2}$$

The $\lambda=+$ and $=-$ branches, with linear dispersion $\varepsilon_{\mathbf{k}\lambda}=\lambda v_F k$, correspond to the conduction and valance bands of the surface states, respectively. Here

$$U(\mathbf{k}) = \frac{1}{\sqrt{2}}\begin{pmatrix} ie^{-i\theta_k} & -ie^{-i\theta_k} \\ 1 & 1\end{pmatrix} \tag{3}$$

are the transform matrices between the collinear and helix spaces, with $\theta_{\mathbf{k}}$ representing the polar angle of the momentum $\mathbf{k}$. The interacting part H_I describes the electron-impurity scattering, electron-phonon coupling, and electron-electron Coulomb interaction. In unit area, it can be written as

$$\begin{aligned} H_I =& \sum_{\mathbf{q},\mathbf{k}\sigma} v_{\mathbf{q}}\rho_I(\mathbf{q})c^\dagger_{\mathbf{k}+\mathbf{q}\sigma}c^\dagger_{\mathbf{k}\sigma} \\ &+ \sum_{\lambda\mathbf{q}\Omega,\mathbf{k}\sigma} M_\lambda(\mathbf{q},\Omega)\phi_\lambda(\mathbf{q},\Omega)c^\dagger_{\mathbf{k}+\mathbf{q}\sigma}c_{\mathbf{k}\sigma} \\ &+ \sum_{\mathbf{q}\mathbf{k}'\sigma'\mathbf{k}\sigma} v_{\mathbf{q}}c^\dagger_{\mathbf{k}'-\mathbf{q}\sigma'}c^\dagger_{\mathbf{k}+\mathbf{q}\sigma}c_{\mathbf{k}\sigma}c_{\mathbf{k}\sigma'}. \end{aligned} \tag{4}$$

Here $v_{\mathbf{q}}=e^2/(2\varepsilon_0\kappa_0 q)$ with e, ε_0, and κ_0 standing for the elementary charge, permittivity, and the dielectric constant of Bi_2Se_3, respectively. $\kappa=100$ [20,25,29]. $\rho_I(\mathbf{q})=\sum_{i=1}^{N_i}e^{i\mathbf{q}\cdot\mathbf{R}_i}$, where $\mathbf{R}_i$ is the position of the ith impurity and N_i is the impurity density. $\phi_\lambda(\mathbf{q},\Omega)=b_\lambda(\mathbf{q},\Omega)+b^\dagger_\lambda(-\mathbf{q},\Omega)$, with $b_\lambda(\mathbf{q},\Omega)$ [$b^\dagger_\lambda(\mathbf{q},\Omega)$] being the annihilation (creation) operators of the phonon with branch λ, momentum $\mathbf{q}$, and energy Ω. For the electron-phonon coupling, we include contributions from the surface optical phonon, and from the longitudinal and transverse acoustic phonons [30].[1] The matrix elements for the electron-surface optical phonon coupling read

$$M_{\rm op}(\mathbf{q},\Omega=\omega_o)=(\lambda_1+\lambda_2 q)/\sqrt{2M\mathcal{A}\omega_o}, \tag{5}$$

where M is the ion mass, $\mathcal{A}$ is the primitive cell area $[1/(M\mathcal{A})=4\times10^{-3}\,\text{meV}]$, $\lambda_1=5\,\text{eV nm}$, $\lambda_2=1.6\,\text{eV nm}^2$, and $\omega_o=8$ meV is the optical phonon energy [2,32]. For the longitudinal and transverse acoustic phonons, the matrix elements of the electron-phonon coupling read

$$M_L(\mathbf{q},\Omega)=-\alpha\frac{(\Omega/v_l)^2}{\sqrt{2\rho_M\Omega}}\frac{\left(q^2-k_t^2\right)^2-4q^2k_lk_t}{\left(q^2-k_t^2\right)^2+4q^2k_lk_t}\Theta(\Omega-v_lq), \tag{6}$$

$$M_T(\mathbf{q},\Omega)=-\alpha\frac{(\Omega/v_l)^2}{\sqrt{2\rho_M\Omega}}\frac{4q\left(q^2-k_t^2\right)\sqrt{k_lk_t}}{\left(q^2-k_t^2\right)^2+4q^2k_lk_t}\Theta(\Omega-v_tq), \tag{7}$$

respectively [30]. In the above equations, $k_{l,t}=\sqrt{(\Omega/v_{l,t})^2-q^2}$, $v_{l(t)}=2900(1700)$ m/s is the longitudinal (transverse) sound velocity [29,33], $\rho_M=7860\,\text{kg/m}^3$ is the mass density [34,35], and $\alpha=70$ eV [30].

By using the nonequilibrium Green function method [36], we construct the KSBEs for spatially uniform system as follows [25,37,38]:

$$\begin{aligned} &\partial_t\rho_{\mathbf{k}}(t)+i[v_Fk\sigma_z,\rho_{\mathbf{k}}(t)]-eE\partial_{k_x}\rho_{\mathbf{k}}(t) \\ &\quad -eE[U^\dagger(\mathbf{k})\partial_{k_x}U(\mathbf{k}),\rho_{\mathbf{k}}(t)]+\partial_t\rho_{\mathbf{k}}(t)|_{\rm scat}=0. \end{aligned} \tag{8}$$

Here $\rho_{\mathbf{k}}(t)$ is the density matrix for electrons with momentum $\mathbf{k}$ in the helix spin space, i.e., the space spanned by the eigenstates of H_0 in Eq. (1). The diagonal elements of $\rho_{\mathbf{k}}(t)$, $\rho_{\mathbf{k}++/--}(t)=f_{\mathbf{k}+/-}(t)$, represent the electron distribution functions in the conduction and valance bands, respectively, while the off-diagonal terms stand for the interband coherence. The KSBEs include the coherent term (the second term in the left-hand side of the equation), the acceleration of the electron under the electric field E (the third term), the interband precession induced by the field (the fourth term) as well as the scattering term (the fifth term). The electric-field-induced interband precession originates from the spin mixing in the conduction and valance bands. A similar effect also exists in graphene where the pseudospins are mixed [39]. This term is usually ignored in the previous studies on low field transport [39]. However, it is shown that the electric-field-induced interband precession has a profound influence on the transport properties under high electric field, as it leads to a strong excitation of the carriers from the surface valance band to the conduction band [25]. The expressions for the scattering term can be found in Ref. [25], which includes the contribution

[1] As in the bulk transport [31], the contribution of the acoustic phonon is also very small compared to the surface transport. The transport relaxation time of electron–acoustic-phonon scattering is about 1% of that of electron-impurity scattering. However, we have to include the acoustic phonon in our calculation, at least in the low field and low temperature regime, in order to obtain the steady state.

from electron-electron Coulomb interaction, electron-impurity scattering, and electron-phonon coupling.

By numerically solving the KSBEs for spatially uniform system, one obtains the charge current density J for the applied electric field E. We apply our results to a sample with length $L = 410$ nm and width $W = 300$ nm, the same length and width as those of the sample D2 in Ref. [24], in order to obtain quantities such as the applied voltage $V = EL$ and the conductance $G = I/V$ with the current $I = 2JW$. Here the prefactor 2 is from the fact that each sample contains two surfaces.

III. NUMERICAL RESULTS

In Fig. 1(a), we plot the current I as a function of the applied voltage V at 4.2 K for the surface states with electron density $N_e = 1.5 \times 10^{11}$ cm^{-2} and impurity density $N_i = 6 \times 10^{11}$ cm^{-2}, which is of same order of magnitude as the surface charge density. One can see that our theoretical results capture all the main experimental results qualitatively. Namely, the current I increases linearly with the increase of the voltage V when the voltage is small. Then the current shows a tendency of saturation at intermediate voltage but increases again when the voltage rises higher than 50 mV. This incomplete saturation can also be seen in the voltage dependence of the conductance G, also shown in Fig. 1(a). One finds from the figure that the conductance decreases as the voltage increases, then saturates to a finite constant under higher voltage.

The decrease of the conductance is a result of the hot-electron effect under high electric field [25,40]. Due to the driving of the electric field, the temperature of the electrons rises well above the lattice one when the field is high enough. As a result, the electron-phonon scattering is profoundly enhanced, consequently the mobility μ decreases. Therefore, the conductance $G = N_e e\mu EW/V$ decreases with the increase of the voltage. When the electric field E is strong enough, the field dependence of the mobility can be roughly estimated as $1/\mu \simeq 1/\mu_0 + \gamma(N_e)E$. Here μ_0 is the linear mobility, which is determined by the impurity scattering when the temperature is smaller than 70 K. $\gamma(N_e)$ is a constant determined by the electron–optical-phonon scattering [25]. When electron–optical-phonon scattering becomes dominant due to the hot-electron effect, which happens when $E >$ 1 kV/cm or $V > 50$ mV in our calculation, the mobility is inversely proportional to E, $1/\mu \simeq \gamma(N_e)E$. One can therefore estimate that the current should saturates to $I_s = N_e eW\gamma(N_e)$ under high voltage. This current saturation can be crudely captured by the so-called steady-state population model with instantaneous phonon emission [41,42].

If the saturation is complete as predicted by the steady-state population model, the current should remain constant and the conductance should approach zero under high voltage. However, our computation shows that under higher applied electric field, the current saturation is not complete. When the voltage further increases the current again rises linearly with the voltage, and the corresponding conductance saturates to a finite value instead of zero. This incomplete current saturation and the finite residual conductance in the high field regime is due to the excitation of carriers from the surface valence band to the surface conduction one via the interband precession (the fourth term in KSBEs), first proposed by Zhang and Wu [25]. In the low field regime, the excitation is proportional to E^2. For sample with a high background carrier density, the number of the excited carriers is too small to have an observable effect on transport properties. In the intermediate regime where

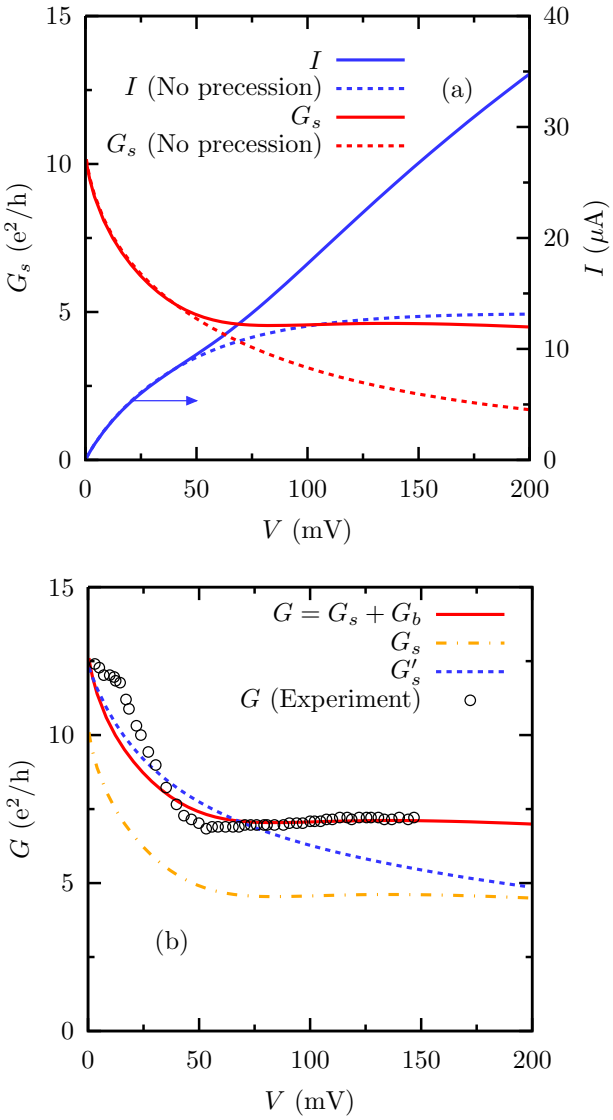

FIG. 1. (Color online) (a) Current (blue curves) and conductance (red curves) as functions of the applied voltage at temperature $T = 4.2$ K for surfaces with $N_e = 1.5 \times 10^{11}$ cm^{-2} and $N_i = 6 \times 10^{11}$ cm^{-2}. The solid and the dashed curves are the results with and without the interband precession. Note that the scale of the current is on the right-hand side of the frame. (b) The conductance as a function of the applied voltage at temperature $T = 4.2$ K with different fitting parameters: The blue dashed curve is the surface conductance G'_s for the surfaces with $N_e = 9.4 \times 10^{11}$ cm^{-2} and $N_i = 2.1 \times 10^{12}$ cm^{-2}. The dark yellow dash-dotted curve is the surface conductance G_s for the surfaces with $N_e = 1.5 \times 10^{11}$ cm^{-2} and $N_i = 6 \times 10^{11}$ cm^{-2}, which is exactly the red solid curve in (a). The red solid curve is the total conductance for the surfaces with $N_e = 1.5 \times 10^{11}$ cm^{-2} and $N_i = 6 \times 10^{11}$ cm^{-2} plus a bulk with a constant conductance $G_b = 2.5e^2/h$. The circles are the experimental data from Ref. [24] for sample D2 under the gate voltage of -120 V.

the mobility is reduced due to the hot-electron effect but the carrier excitation is not yet strong enough, the current shows a tendency of saturation as the mobility decreases. In the higher field regime, when more carriers are excited, the current increases again with the increase of the field. Under strong field, the excited carrier density is proportional to the electric field E, and the total number of the carriers becomes

$$N_e(E) \simeq N_e + \beta E, \tag{9}$$

with β being a constant. Combining with the fact that the mobility is inversely proportional to E in this regime, one finds that the conductance

$$G \simeq [N_e + \beta E] e\mu_0 W/[(1 + \gamma(N_e)\mu_0 E)L]. \tag{10}$$

It is therefore understood that under strong applied electric field/voltage when the number of the excited carriers exceeds the background one, the conductance becomes a finite constant,

$$G_r \simeq \beta e W/[\gamma(N_e)L]. \tag{11}$$

The saturated field E_s is determined by the equation $\beta E_s = N_e$, i.e., when the number of the excited carriers becomes the same as the background one. One can then write down the saturated voltage V_s as

$$V_s = E_s L = N_e L/\beta, \tag{12}$$

which is proportional to the background surface charge density.

If there is no such excitation, the current saturation in the high applied field/voltage regime is complete and the conduction approaches zero. This is verified by our numerical solution, also shown in Fig. 1, with the interband precession term in the KSBEs artificially removed.

To check the quantitative agreement between the experimental results and the theoretical ones, we plot our numerical fittings to the experimental data from Ref. [24] for sample D2 under a gate voltage of -120 V by using different parameters in Fig. 1(b). The electron density per surface is estimated to be 9.4×10^{11} cm^{-2} in the experiment at such a gate voltage. If all the electrons occupy the surface states and the bulk does not have any contribution to the charge transport, then the total conductance G is the same as the surface one. Under this assumption, the surface conductance from our computation (G_s'), shown in Fig. 1(b) as a dashed curve, fits reasonably well with the experimental data in the low field regime when the impurity density is 2.1×10^{12} cm^{-2}. In the high field regime, however, the theoretical results deviate from the experimental ones. The theoretical saturated voltage in this case is about 200 mV, much larger than 50 mV from the experiment, and the residual conductance is about $5e^2/h$, 30% smaller than the experimental one.

According to Eq. (12), to have a smaller saturated voltage, the background surface charge density should be smaller. The overall quantitative fitting can indeed be improved if some of the electrons are assumed to be populated in the bulk impurity bands [23,24]. In this case, the total conductance G is the summation of surface conductance G_s and the bulk one G_b. Since the conductance of the bulk impurity bands is determined by the disorder, G_b can be regarded as a constant that does not variate with the applied voltage in the observed regime [23,24]. In Fig. 1(b) we further show the total conductance G for the surfaces with $N_e = 1.5 \times 10^{11}$ cm^{-2} and $N_i = 6 \times 10^{11}$ cm^{-2} plus a bulk contribution with a constant conductance $G_b = 2.5e^2/h$. One finds that our numerical results are in good agreement with the experimental data for both low and high applied voltages except for the small discrepancy for $V < 30$ mV. It is noted that we do not consider the excitation of carriers from the surface states to the bulk ones in our calculation. The charge densities on the surface and in the bulk remain constant and do not change with the applied field/voltage. Since the bulk charge density and the conductance G_b are constant, all the variations in the transport properties are caused solely by the carriers on the surface. Our results suggest that the bulk indeed has a non-negligible contribution to the total conductance. However, the main transport phenomena, such as the incomplete current saturation and the finite residual conductance under high field, can be understood within the framework of surface transport alone without the influence of the bulk part.

In the works of Checkelsky *et al.* [23] and Costache *et al.* [24], the incomplete current saturation and the finite residual conductance were speculated to be associated with the excitation of the carrier from surface states to the bulk ones which have finite constant conductance. It is argued that in the experimental setup, the energy gap of Bi_2Se_3 can be reduced from 300 meV to about 50 meV due to band bending, thus enabling the carriers on the surface to be excited to the bulk with an applied voltage of 50 mV. For the argument to be valid, the transport must be nearly ballistic so that the carriers in the surface states can gain enough energy to jump over the energy gap. However, in the experimental setup the mean free path is less than 30 nm. It means that the average energy gain by the carriers is less than 4 meV for an applied voltage of 50 mV over a sample with a length of 410 nm. This energy gain is too small to excite the carriers from the surface states to the bulk ones even if the energy gap is indeed reduced to 50 meV. Therefore, the excitation from the surface states to the bulk ones is very unlikely to be the main reason for the incomplete current saturation and the finite residual conductance under high voltage. From our theoretical results, the more likely reason for these high field/voltage transport phenomena is the joint effects of the hot-electron transport and the excitation within the surface bands.

In Fig. 2, we further present the surface conductance as functions of the applied voltage at different temperatures for the same surface as in Fig. 1(a). One can see from the figure that the qualitative behaviors of the surface conductance G_s are the same for all temperatures. The conductance first decreases due to the hot-electron effect as the voltage increases. It then approaches the finite residual values when the voltage becomes larger than 50 mV as the number of the carrier excited from the surface valence band to the surface conduction band exceeds the background one. In the low field regime, the conductance is very sensitive to the temperature. When temperature increases from 4.2 K to 70 K, the linear conductance G_s reduces from $10e^2/h$ to $3.7e^2/h$. On the other hand, the residual conductance in the high field regime is less sensitive to the temperature. When temperature increases from 4.2 K to 70 K, the residual surface conductance varies from $4.6e^2/h$ to $2.9e^2/h$.

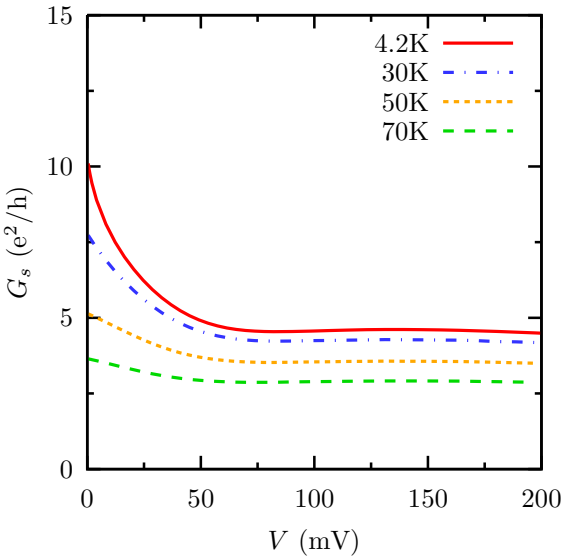

FIG. 2. (Color online) The surface conductance G_s as function of the applied voltage for surfaces with $N_e = 1.5 \times 10^{11}$ cm^{-2} and $N_i = 6 \times 10^{11}$ cm^{-2} at different temperatures: Red solid curve, $T =$ 4.2 K. Blue dash-dotted curve, $T = 30$ K. Dark yellow short-dashed curve, $T = 50$ K. Green long-dashed curve, $T = 70$ K.

The temperature dependence of the conductance is mostly determined by the electron–optical-phonon scattering in the linear transport regime. In this regime, the electron temperature is close to the lattice temperature and the contribution of the electron-optical phonon scattering to the electric resistance is proportional to the number of the optical phonons, $1/(e^{\omega_o/T} - 1)$. Therefore the linear conductance G_s is strongly temperature dependent. In the high field regime, the electron temperature T_e, which is much higher than the lattice temperature T due to the hot-electron effect, has a stronger effect on the strength of the electron-optical phonon scattering than T does. Therefore, the residual conductance in the high field regime becomes less sensitive to T compared to the linear one.

The temperature dependence of our numerical results is in qualitative agreement with the experimental one. However, obtaining good quantitative agreements between the theoretical and experimental results beyond $T = 20$ K is challenging due to many unknown factors at high temperature. In the experiments, the carrier density is controlled by the gate voltage and the capacity. Since the capacity is temperature dependent, the carrier density under different temperatures are different even when the gate voltage remains the same. Moreover, the carriers in the remnant electron pockets can be thermally excited or electrically excited to the bulk conduction band. This effect can enhance the bulk conductance when the temperature or the applied voltage increases [23,24]. As a result, the bulk conductance also depends on the temperature and the applied voltage. Note that if this effect is included, the decrease rate of the total conductance against the applied voltage will become flatter and the small discrepancy between the theoretical and experimental results in Fig. 1(b) for $V < 30$ mV can be further reduced. Furthermore, in the high field regime, the nonequilibrium optical phonon effect can also change the temperature dependence of the conductance [43,44]. To include this effect, knowledge about the scattering between optical and acoustic phonons is required. Due to these unknown factors, more experimental investigations are needed in order to obtain a full understanding of the experimental results at high temperature.

IV. CONCLUSION

In conclusion, we have studied the charge transport on the surface of Bi_2Se_3 by numerically solving the KSBEs and reproduced the main qualitative features of the experimental results, i.e., the incomplete current saturation and the finite residual conductance in the high applied voltage regime, without introducing any bulk contribution. Due to the hot-electron effect, the electron-phonon scattering is enhanced and leads to a reduced mobility, inversely proportional to the applied field in the high field regime. As a result, the current shows a tendency of saturation. On the other hand, the applied electric field can excite carriers from the surface valance band to the surface conduction one due to the interband precession. This leads to the increase of the current carrying carriers and thus the increase of current. Under high applied voltage, the conductance approaches a finite residual value as the number of the excited carriers, being proportional to the electric field, exceeds the background one. Moreover, the theoretical results agree quantitatively well with the experimental data if a constant bulk conductance, which does not change with the applied voltage in the experimentally measured regime, is introduced. This suggests that even though the bulk has a non-negligible contribution to the the total conductance, the main transport phenomena, such as the incomplete current saturation and the finite residual conductance at high applied voltage/field, can be well understood in the framework of surface transport alone.

ACKNOWLEDGMENTS

This work was supported by the National Natural Science Foundation of China under Grant No. 11334014, the National Basic Research Program of China under Grant No. 2012CB922002, and the Strategic Priority Research Program of the Chinese Academy of Sciences under Grant No. XDB01000000.

[1] L. Fu, C. L. Kane, and E. J. Mele, Phys. Rev. Lett. **98**, 106803 (2007).
[2] H. Zhang, C.-X. Liu, X.-L. Qi, X. Dai, Z. Fang, and S.-C. Zhang, Nat. Phys. **5**, 438 (2009).
[3] Y. Xia, D. Qian, D. Hsieh, L. Wray, A. Pal, H. Lin, A. Bansil, D. Grauer, Y. S. Hor, R. J. Cava, and M. Z. Hasan, Nat. Phys. **5**, 398 (2009).
[4] D. Hsieh, Y. Xia, D. Qian, L. Wray, F. Meier, J. H. Dil, J. Osterwalder, L. Patthey, A. V. Fedorov, H. Lin, A. Bansil, D. Grauer, Y. S. Hor, R. J. Cava, and M. Z. Hasan, Phys. Rev. Lett. **103**, 146401 (2009).
[5] M. Z. Hasan and C. L. Kane, Rev. Mod. Phys. **82**, 3045 (2010).
[6] D. Hsieh, Y. Xia, D. Qian, L. Wray, J. H. Dil, F. Meier, J. Osterwalder, L. Patthey, J. G. Checkelsky, N. P. Ong,

A. V. Fedorov, H. Lin, A. Bansil, D. Grauer, Y. S. Hor, R. J. Cava, and M. Z. Hasan, Nature (London) **460**, 1101 (2009).
[7] J. G. Analytis, R. D. McDonald, S. C. Riggs, J.-H. Chu, G. S. Boebinger, and I. R. Fisher, Nat. Phys. **6**, 960 (2010).
[8] Z.-H. Pan, E. Vescovo, A. V. Fedorov, D. Gardner, Y. S. Lee, S. Chu, G. D. Gu, and T. Valla, Phys. Rev. Lett. **106**, 257004 (2011).
[9] Y. L. Chen, J. G. Analytis, J.-H. Chu, Z. K. Liu, S.-K. Mo, X. L. Qi, H. J. Zhang, D. H. Lu, X. Dai, Z. Fang, S. C. Zhang, I. R. Fisher, Z. Hussain, and Z.-X. Shen, Science **325**, 178 (2009).
[10] X.-L. Qi and S.-C. Zhang, Rev. Mod. Phys. **83**, 1057 (2011).
[11] M. Z. Hasan and J. E. Moore, Annu. Rev. Condens. Matter Phys. **2**, 55 (2011).
[12] X.-L. Qi, T. L. Hughes, and S.-C. Zhang, Phys. Rev. B **78**, 195424 (2008).
[13] G. A. Fiete, V. Chua, M. Kargarian, R. Lundgren, A. Rüegg, J. Wen, and V. Zyuzin, Physica E **44**, 845 (2012).
[14] D. Culcer, Physica E **44**, 860 (2012).
[15] D. Culcer, E. H. Hwang, T. D. Stanescu, and S. Das Sarma, Phys. Rev. B **82**, 155457 (2010).
[16] A. A. Burkov and D. G. Hawthorn, Phys. Rev. Lett. **105**, 066802 (2010).
[17] H.-Z. Lu and S.-Q. Shen, Phys. Rev. Lett. **112**, 146601 (2014).
[18] L. Barreto, L. Kühnemund, F. Edler, C. Tegenkamp, J. Mi, M. Bremholm, B. B. Iversen, C. Frydendahl, M. Bianchi, and P. Hofmann, Nano Lett. **14**, 3755 (2014).
[19] B. Skinner, T. Chen, and B. I. Shklovskii, JETP **117**, 579 (2013).
[20] N. P. Butch, K. Kirshenbaum, P. Syers, A. B. Sushkov, G. S. Jenkins, H. D. Drew, and J. Paglione, Phys. Rev. B **81**, 241301 (2010).
[21] J. G. Analytis, J.-H. Chu, Y. Chen, F. Corredor, R. D. McDonald, Z. X. Shen, and I. R. Fisher, Phys. Rev. B **81**, 205407 (2010).
[22] K. Eto, Z. Ren, A. A. Taskin, K. Segawa, and Y. Ando, Phys. Rev. B **81**, 195309 (2010); Z. Ren, A. A. Taskin, S. Sasaki, K. Segawa, and Y. Ando, *ibid.* **84**, 075316 (2011); **84**, 165311 (2011); **85**, 155301 (2012).
[23] J. G. Checkelsky, Y. S. Hor, R. J. Cava, and N. P. Ong, Phys. Rev. Lett. **106**, 196801 (2011).
[24] M. V. Costache, I. Neumann, J. F. Sierra, V. Marinova, M. M. Gospodinov, S. Roche, and S. O. Valenzuela, Phys. Rev. Lett. **112**, 086601 (2014).
[25] P. Zhang and M. W. Wu, Phys. Rev. B **87**, 085319 (2013).
[26] Y. A. Bychkov and E. I. Rashba, J. Phys. C **17**, 6039 (1984).
[27] C.-X. Liu, X.-L. Qi, H. Zhang, X. Dai, Z. Fang, and S.-C. Zhang, Phys. Rev. B **82**, 045122 (2010).
[28] L. Fu, Phys. Rev. Lett. **103**, 266801 (2009).
[29] W. Richter and C. R. Becker, Phys. Status Solidi B **84**, 619 (1977).
[30] S. Giraud and R. Egger, Phys. Rev. B **83**, 245322 (2011); S. Giraud, A. Kundu, and R. Egger, *ibid.* **85**, 035441 (2012).
[31] F. Rittweger, N. F. Hinsche, P. Zahn, and I. Mertig, Phys. Rev. B **89**, 035439 (2014).
[32] X. Zhu, L. Santos, R. Sankar, S. Chikara, C. Howard, F. C. Chou, C. Chamon, and M. El-Batanouny, Phys. Rev. Lett. **107**, 186102 (2011).
[33] G. E. Shoemake, J. A. Rayne, and R. W. Ure, Phys. Rev. **185**, 1046 (1969).
[34] J. Wiese and L. Muldawer, J. Phys. Chem. Solids **15**, 13 (1960).
[35] L. Fu and C. L. Kane, Phys. Rev. B **76**, 045302 (2007).
[36] H. Haug and A.-P. Jauho, *Quantum Kinetics in Transport and Optics of Semiconductors* (Springer, Berlin, 1996).
[37] M. W. Wu, J. H. Jiang, and M. Q. Weng, Phys. Rep. **493**, 61 (2010).
[38] J. L. Cheng and M. W. Wu, J. Appl. Phys. **99**, 083704 (2006).
[39] O. G. Balev, F. T. Vasko, and V. Ryzhii, Phys. Rev. B **79**, 165432 (2009).
[40] M. Q. Weng, M. W. Wu, and L. Jiang, Phys. Rev. B **69**, 245320 (2004).
[41] A. Barreiro, M. Lazzeri, J. Moser, F. Mauri, and A. Bachtold, Phys. Rev. Lett. **103**, 076601 (2009).
[42] Z. Yao, C. L. Kane, and C. Dekker, Phys. Rev. Lett. **84**, 2941 (2000).
[43] P. Zhang and M. W. Wu, Europhys. Lett. **92**, 47009 (2010).
[44] X. L. Lei and N. J. M. Horing, Phys. Rev. B **35**, 6281 (1987).